

# Impact of the arc length on GNSS analysis results

Simon Lutz<sup>1</sup> · Michael Meindl<sup>2</sup> · Peter Steigenberger<sup>3</sup> · Gerhard Beutler<sup>4</sup> ·  
Krzysztof Sośnica<sup>4,5</sup> · Stefan Schaer<sup>1</sup> · Rolf Dach<sup>4</sup> ·  
Daniel Arnold<sup>4</sup> · Daniela Thaller<sup>6</sup> · Adrian Jäggi<sup>4</sup>

Received: 6 May 2015 / Accepted: 1 December 2015  
© Springer-Verlag Berlin Heidelberg 2015

**Abstract** Homogeneously reprocessed combined GPS/GLONASS 1- and 3-day solutions from 1994 to 2013, generated by the Center for Orbit Determination in Europe (CODE) in the frame of the second reprocessing campaign REPRO-2 of the International GNSS Service, as well as GPS- and GLONASS-only 1- and 3-day solutions for the years 2009 to 2011 are analyzed to assess the impact of the arc length on the estimated Earth Orientation Parameters (EOP, namely polar motion and length of day), on the geocenter, and on the orbits. The conventional CODE 3-day solutions assume continuity of orbits, polar motion components, and of other parameters at the day boundaries. An experimental 3-day solution, which assumes continuity of the orbits, but independence from day to day for all other parameters, as well as a non-overlapping 3-day solution, is included into our analysis. The time series of EOPs, geocenter coordinates, and orbit misclosures, are analyzed. The long-arc solutions

were found to be superior to the 1-day solutions: the RMS values of EOP and geocenter series are typically reduced between 10 and 40%, except for the polar motion rates, where RMS reductions by factors of 2–3 with respect to the 1-day solutions are achieved for the overlapping and the non-overlapping 3-day solutions. In the low-frequency part of the spectrum, the reduction is even more important. The better performance of the orbits of 3-day solutions with respect to 1-day solutions is also confirmed by the validation with satellite laser ranging.

**Keywords** GPS · GLONASS · Orbits · Earth orientation parameters

## 1 Motivation and introduction

When analyzing data from a globally distributed network of GNSS receivers over a certain time span, e.g., one or several days, one has to solve a complex parameter estimation problem with many parameter types, including in particular orbit and Earth orientation parameters (EOP). Orbit parameters include the initial position and velocity vectors, scale parameters of perturbing accelerations, e.g., of a solar radiation pressure model, and/or empirical parameters like instantaneous velocity changes. Different analysis groups of the International GNSS Service (IGS, [Dow et al. 2009](#)) use different approaches. Concerning the EOPs it has become standard to model polar motion in the coordinates  $x$  and  $y$  and UT1-UTC as linear over 1 day.

Using the estimates of the pole coordinates  $x$  and  $y$  referring to noon (GPS time) and of their rates  $\dot{x}$  and  $\dot{y}$ , valid for the entire day, one may calculate the pole coordinates  $x$  and  $y$  at any time, in particular at the day boundaries. For the boundary between days  $i$  and  $i + 1$ , one may calculate the

✉ Simon Lutz  
simon.lutz@swisstopo.ch

<sup>1</sup> Federal Office of Topography (swisstopo),  
Seftigenstrasse 264, 3084 Wabern, Switzerland

<sup>2</sup> Institute of Geodesy and Photogrammetry, ETH Zürich,  
Robert-Gnehm-Weg 15, 8093 Zurich, Switzerland

<sup>3</sup> Deutsches Zentrum für Luft- und Raumfahrt, German Space  
Operations Center, Münchener Straße 20, 82234 Weßling,  
Germany

<sup>4</sup> Astronomical Institute, University of Bern, Sidlerstrasse 5,  
3012 Bern, Switzerland

<sup>5</sup> Institute of Geodesy and Geoinformatics, Wrocław University  
of Environmental and Life Sciences, Grunwaldzka 53,  
50–357 Wrocław, Poland

<sup>6</sup> Bundesamt für Kartographie und Geodäsie,  
Richard-Strauss-Allee 11, 60598 Frankfurt am Main,  
Germany

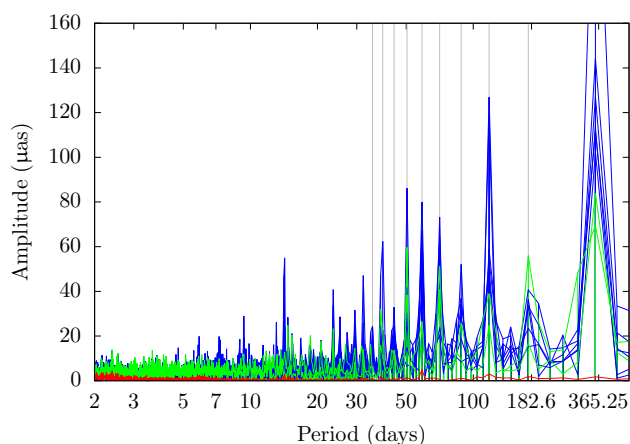


**Fig. 1** Amplitude spectra of  $y$ -pole coordinate misclosures from REPRO-2 series in 2009–2013 for six 1-day solutions (blue), two 30-h solutions (green), and a 3-day solution (red). The vertical gray lines mark the harmonics of the GLONASS draconitic year

position of the pole using the parameters of either day  $i$  or  $i + 1$ . It is thus possible to define a misclosure of the pole coordinates. For  $y$  we have

$$\Delta y_{i,i+1} = y_i + \frac{1}{2} \dot{y}_i - \left( y_{i+1} - \frac{1}{2} \dot{y}_{i+1} \right), \quad i = 1, 2, \dots \quad (1)$$

Figure 1, showing the spectra of the  $y$ -pole misclosures in the time interval 2009–2013 for all Analysis Centers (AC) contributing to the reprocessing campaign REPRO-2 of the IGS<sup>1</sup>, illustrates that there is a problem: the spectra associated with the six 1-day solutions contain spectral lines with large amplitudes at the harmonic periods of either the draconitic GPS annual period of 351.5 days and/or the draconitic GLONASS annual period of 353.2 days.<sup>2</sup> The 30-h solutions show somewhat smaller amplitudes compared to the true 1-day solutions. However, only the 3-day solution<sup>3</sup> does not show any significant amplitudes. There are pure GPS and combined GPS/GLONASS solutions among the 1-day solutions of Fig. 1. Obviously, the problem is not restricted to solutions using GLONASS. The differences  $\Delta x_{i,i+1}$  show a comparable pattern as the  $y$ -component.

The problem of pole misclosures resides in the correlation of the motion of the pole within the day with the orbital elements of the satellites. Hefty et al. (2000) showed that special techniques (“blocking retrograde diurnal terms”) had to be applied to render the solution with a sub-daily resolution

of polar motion regular. Solving for pole offsets and rates is the simplest case of sub-daily polar motion resolution. This particular problem is not singular, but it is not well posed, either. The method proposed by Hefty et al. (2000) to remove the singularity is not helpful in this context, because it would result in constraining the polar motion rates to zero. The CODE<sup>4</sup> 3-day solution (red line in Fig. 1) underscores that the correlation problem is substantially reduced when replacing the 1- by a 3-day solution.

Subsequently, we focus on the impact of the arc length on geophysically relevant parameters when using the Extended CODE Orbit Model (ECOM) developed by Springer et al. (1999). This orbit model was improved by Arnold et al. (2015), where one can also find an up-to-date description of both, the old and new ECOM. The old model is used here, because it is underlying all CODE solutions in the REPRO-2 campaign. Strictly speaking, the presented results, therefore, only apply to ECOM-type orbit models. The arc length will not be treated as a “continuous” parameter. For practical and pragmatic reasons, only 1- and 3-day solutions are discussed.

Section 2 gives an overview of previous works relevant in the context. Section 3 briefly introduces the sets of GNSS observations, the GNSS analysis procedures, and the different solution series used in this article. Section 4 discusses GNSS-specific 1- and 3-day solutions based on data of the years 2009–2011. Section 5 analyzes the results of a 1-day and two different 3-day combined GPS/ GLONASS solutions covering more than 10 years. Section 6 discusses the quality of EOPs and geocenter coordinates based on non-overlapping 3-day solutions. In Sect. 7, two of the solution series are validated with the Satellite Laser Ranging (SLR) technique. Section 8 summarizes the results and draws the conclusions.

## 2 Survey of previous works

Our EOP series will be compared to the products of the IERS (International Earth Rotation and Reference Systems Service, Dick and Thaller 2014). Gambis (2004) describes the background of generating the IERS combined EOP series C04. The principles laid down in that article are still valid today. The pole coordinates  $x$  and  $y$ , UT1-UTC and length of day (LOD), as well as the associated error information are made available with a daily spacing at midnight of each day since January 1, 1962. The IERS 08 C04 series is based on contributions from VLBI<sup>5</sup>, SLR, GPS (today in fact GNSS,

<sup>1</sup> Summaries of the analysis strategies for each AC can be found at <http://acc.igs.org/reprocess2.html>.

<sup>2</sup> The draconitic year of a satellite represents the revolution period of the Sun with respect to its orbital plane.

<sup>3</sup> The 3-day solution is the C3 solution defined in Sect. 3.

<sup>4</sup> CODE, the Center for Orbit Determination in Europe, is a joint venture of the Astronomical Institute, University of Bern (AIUB), the Federal Office of Topography (swisstopo), the Bundesamt für Kartographie und Geodäsie (BKG), and the Institut für Astronomische und Physikalische Geodäsie, Technische Universität München (TUM).

<sup>5</sup> Very Long Baseline Interferometry.

i. e., GPS and GLONASS), and DORIS<sup>6</sup> and is consistent with the current version of the International Terrestrial Reference Frame, namely ITRF2008 (Altamimi et al. 2011). The solutions of CODE were included for the parameters  $x$ ,  $y$ , and LOD via the IGS combination, implying that our series are not fully independent of the C04 series.

Subsequently, we will frequently refer to large systematic errors with annual, semiannual, etc. periods introduced into parameters of geophysical interest by orbit modeling deficiencies. The articles Ray et al. (2008), Griffiths and Ray (2012), and Ray et al. (2013) are relevant in this context. The first reference describes spurious spectral lines in the IGS station coordinates as early as 2008, based on GNSS results at a time when GLONASS did not yet play a significant role in the IGS network. The periods of the spectral lines could be attributed to the draconitic GPS year. The effects are small, but detectable. The second reference states that draconitic errors are contained in virtually all IGS products, not only in the station coordinates. The third gives an update on the analysis of these spurious effects. It is pointed out that all IGS analysis centers show in addition fortnightly periods in their results.

Our analysis is not based on the operational products of CODE, but on homogeneous solutions generated with one and the same set of background models and station coordinates. Steigenberger et al. (2006) define GNSS data modeling by specifying the background models, parameter space, and the constraints set up in the analysis, as well as the processing scheme including aspects like ambiguity resolution and the length of the orbital arcs. The study was based on GPS data from 1994 to 2003 and it is broad in scope by including, e. g., EOPs with a 1-h time resolution. The Bernese GNSS Software (Dach et al. 2007) was used for the analysis.

The references discussed so far did not consider the arc length as a selectable parameter of orbit modeling and GNSS analysis. This aspect is in the focus of our study.

### 3 Global data sets and solution series

Table 1 gives an overview of the solutions analyzed. The first group was originally generated by Meindl (2011), using 92 sites of the global network that are equipped with well-performing combined GPS/GLONASS receivers, where the time interval 2008–2010 was studied. The series were extended by adding the year 2011 (Meindl et al. 2013) and the 3-day solutions were generated exclusively for the present article. The G1/G3 and R1/R3 solutions were generated in the same way as the C1 and C3 solutions (descriptions below), except that only GPS or GLONASS observations

**Table 1** Solution series characteristics

Solution	Data span	Description
G1/G3	2008–2011	GPS-only, 1- and 3-day
R1/R3	2008–2011	GLONASS-only, 1- and 3-day
C1/C3	1994–2013	Combined, 1- and 3-day
Cx	1994–2013	Combined, 3-day orbits but otherwise 1-day products
Cn	1994–2013	Reconstructed from C3, non-overlapping 3-day solution

were used, respectively. This set of solutions will be analyzed in Sect. 4.

The second set of solutions is based on the IGS tracking network as analyzed in CODE REPRO-2 covering the years 1994–2013. More than 200 sites were available each day at the end of the time interval. Note that GLONASS has only been included since 2002. The principles of the data analysis are the same as those underlying Steigenberger et al. (2006). The CODE contribution to the first IGS reprocessing REPRO-1 is discussed in full detail by Steigenberger et al. (2011), modifications for REPRO-2 are available electronically.<sup>7</sup>

C1 is the 1-day product based on the observations of exactly one calendar day in GPS time (close to UTC). Six initial osculating orbital elements, five parameters of the ECOM, and one (instantaneous) velocity change in the along-track direction at noon serve as orbit parameters for each satellite. Note, however, that the G1/G3 and R1/R3 solutions were generated without the noon pulses. The  $x$ - and  $y$ -coordinates of the pole and UT1-UTC are allowed to change linearly over the day. The first estimated value for UT1-UTC is constrained to the a priori value from the IERS in all 1- and 3-day solutions. Diurnal and sub-diurnal variations in polar motion and UT1-UTC are applied as background models specified in the IERS conventions (Petit and Luzum 2010). The coordinates of the tracking sites are assumed constant over the day. For further details of the processing consult Dach et al. (2009).

The C3 series is based on the daily C1 NEQs (Normal Equation Systems) of three consecutive days, which are superimposed using the methodology documented by Beutler et al. (1996) and Brockmann (1997). The C3 solution solves for one set of site coordinates over the 3 days, makes the EOPs continuous at the boundaries of the middle day, but allows for instantaneous changes in the rates by a piece-wise linear representation with nodal points at midnight. The orbital arcs resulting from the C3 solution are continuous over 3 days but

<sup>6</sup> Doppler Orbitography and Radiopositioning Integrated by Satellite.

<sup>7</sup> Summary of the analysis strategy: [ftp://ftp.unibe.ch/aiub/REPRO\\_2013/CODE\\_REPRO\\_2013.ACN](ftp://ftp.unibe.ch/aiub/REPRO_2013/CODE_REPRO_2013.ACN).

allow for instantaneous velocity changes at all noon and midnight epochs in GPS time using constraints as documented by Dach et al. (2009).

Cx is a hybrid solution sitting in between the C1 and C3 solutions. It is also based on the C1 NEQs of three subsequent days, but no continuity is imposed for any parameter type except for the orbits. The Cn series is based on C3, but makes use of only every third solution, thus, without overlaps. The time resolution of the geocenter coordinate time series is, therefore, 3 days. For the EOPs, however, 1-day values are extracted at noon from the (daily) continuous piece-wise linear parameters. All solutions analyzed in this study are based on the 5-parameter ECOM. The observations of GPS and GLONASS are given the same weight. The initially small number of GLONASS observations, however, gave GLONASS a smaller weight in the early years.

## 4 Single-system 1- and 3-day solutions

### 4.1 The geocenter estimates

According to Meindl et al. (2013) the geocenter is the vector of the Earth's center of mass with respect to the origin of the terrestrial network. Its coordinates can be determined with satellite-geodetic methods. As the geocenter estimates of 1-day GNSS solutions were extensively studied by Meindl et al. (2013), we focus on the 3-day results and put them in relation to the 1-day results.

The geocenter  $x$ -,  $y$ -, and  $z$ -components have been spectrally analyzed. The zero-order term of the Fourier series expansion, i.e., the offset of the geocenter solution with respect to the ITRF2008, is small for all solutions: 3, 5, and 8 mm for the  $x$ -,  $y$ -, and  $z$ -offsets. Except for the  $y$ -component the offsets are even smaller for the 1- than the 3-day solutions. Offsets and phases of the same order of magnitude are seen by the SLR technique (Sośnica et al. 2013).

The GLONASS-only 1-day solution is dominated by the amplitude of 112 mm at 3 cpy (cycles per year) in the  $z$ -coordinate. This amplitude is reduced by about 10% in the GLONASS-only 3-day solution. The amplitudes of  $\geq 32$  mm in  $z$  at 1 cpy and of  $\geq 10$  mm at 2 and 4 cpy are also too large to be real. These amplitudes are not reduced in the 3-day solutions. Moreover, GPS and GLONASS provide substantially different  $z$ -coordinates of the geocenter.

As opposed to the  $z$ -component, the amplitudes in the  $x$ - and  $y$ -components of the geocenter are clearly reduced at 1 cpy when switching from 1- to 3-day arcs and they come close to the amplitudes reported by SLR. As recent results show, the phases of the annual signals from GNSS and SLR agree quite well for the  $x$ - and  $y$ -components of the

**Table 2** Effect of the arc length on the RMS of the geocenter series 2009–2011; units are mm

Periods included	Coord	R1	G1	R3	G3
All	$x$	13	8	9	6
	$y$	10	11	8	7
	$z$	103	12	95	9
<30 days	$x$	9	4	6	3
	$y$	8	5	5	3
	$z$	22	7	18	4
>30 days	$x$	13	8	9	6
	$y$	10	11	8	7
	$z$	101	9	93	8

geocenter, but not for the  $z$ -component (Rebischung et al. 2015).

While the GNSS-specific differences are obvious in the  $z$ -coordinates of the geocenter, they are more difficult to characterize in the other two components. The RMS of the geocenter coordinate series helps to get more insight. The RMS of discrete time series is defined as the square root of the mean value of the squares of all terms of the series. By virtue of Parseval's theorem (Press et al. 1996) the RMS may also be computed using the amplitudes of the Fourier expansion. When including only the terms with periods above a certain threshold, one characterizes the noise in the low-frequency domain (low-pass part of the series), and when including the terms below a certain threshold, one characterizes the noise in the high-frequency domain (high-pass part of the series).

Table 2 illustrates the impact of the arc length on the geocenter solution series when using the RMS values as a criterion. Three sets of RMS values are provided: the full RMS using the amplitudes associated with all periods, the high-pass RMS when including the amplitudes at periods shorter than 30 days, and the low-pass part of the RMS when including the amplitudes at periods longer than 30 days. The threshold of 30 days was selected to include most of the harmonics of the draconitic year in the low-pass part and to assign the tidal periods to the high-pass part.

The total RMS in Table 2 is dominated by the low-pass part (compare first and last part of the table). The high-pass RMS of the 3-day series is about a factor of  $\sqrt{3}$  smaller than the corresponding RMS of the 1-day series. This improvement has to be expected, because the geocenter coordinates of the 3-day solutions contain three times as many observations than those of the 1-day solutions. The central part of the table, therefore, nicely shows that the 3-day solutions for the geocenter are in essence low-pass filtered versions of the 1-day solutions (corresponding to a moving average over 3 days). Table 2 also shows, however, that the RMS values of the low-pass part of the series (in view of the above remark

thus also of the total RMS) substantially improves with the arc length. This gain, ranging between 20 and 36 % in the  $x$ - and  $y$ -coordinates and around 10 % in the  $z$ -coordinate can be attributed to the arc length. The relative gain in the low-pass part is about the same for the GPS and GLONASS solutions.

#### 4.2 The EOP estimates

The polar motion parameters  $x$ ,  $y$ ,  $\dot{x}$ , and  $\dot{y}$ , and the LOD values are compared to the corresponding values of the IERS 08 C04 series (Bizouard and Gambis 2009). The IERS 08 C04 series provides daily values at 0h, whereas all IGS-related products refer to 12h UTC. Therefore, one series has to be interpolated to the time arguments of the other. Interpolating polynomials of degree 3 turned out to be sufficient for that purpose. As no polar motion rates  $\dot{x}$  and  $\dot{y}$  are available in the C04 series, they had to be calculated by taking the first time derivative of the interpolating polynomials.

Three kinds of LOD values may be extracted from the C04 series: one based directly on the LOD values, one using the differences of the UT1-UTC values of two subsequent midnight epochs, and one derived from the first derivative of the interpolating polynomial of the UT1-UTC values. Our LOD values will be compared to the UT1-UTC differences from C04. These are mainly derived from VLBI and thus are to a high degree independent of GNSS. GNSS is only used to improve the high-frequency variations in the C04 UT1-UTC values (Gambis and Luzum 2011).

At the epochs, when the Sun crosses the orbital planes, the GLONASS-derived differences of  $\dot{y}$  in the 1-day solution in Fig. 2 change rapidly by up to 2 mas/day. As the changes always occur when the elevation angle of the Sun above the satellites' orbital planes is close to zero, the variations must be related to deficiencies of the GLONASS radiation pressure model. The same pattern of systematics as seen in  $\dot{y}$  for GLONASS is also visible in the  $x$ -component of the GLONASS-derived polar motion. The rapid changes of about 2 mas/day in the 1-day  $y$ -rates are, however, reduced to about 0.5 mas in the pole coordinates.

As in the case of  $\dot{y}$  and  $x$ , we have seen a similarity in the patterns of  $\dot{x}$  and  $y$ , which may be expected because in a circular polar motion of angular velocity  $\omega$  one has:  $\dot{x} = -\omega y$  and  $\dot{y} = +\omega x$ .

The mean errors of the EOPs are reduced by a factor of about 4 when switching from 1- to 3-day arcs in the case of GLONASS. As there are three times more observations available in the 3-day arc, one would expect an error reduction of about  $\sqrt{3}$ . The much better reduction factor must, therefore, be attributed to a significant reduction of correlations between parameters in the 3-day solutions, which is due, in turn, to the continuity of orbits and EOPs over 3 days.

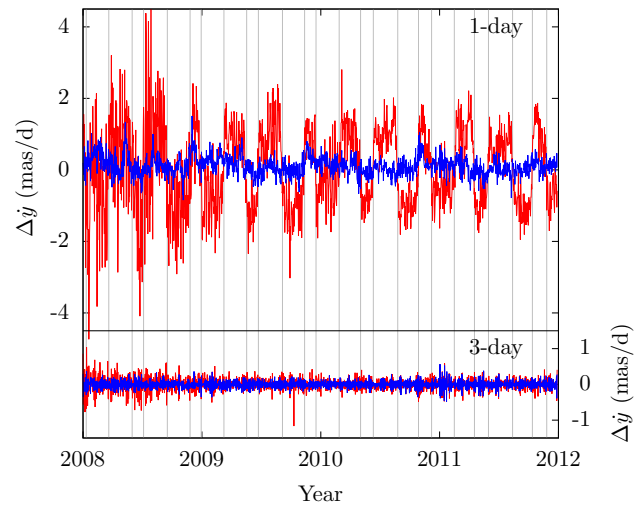


**Fig. 2** Polar motion rate  $\dot{y}$  differences of GLONASS (red) and GPS (blue) 1- and 3-day solutions with respect to IERS 08 C04. The gray vertical lines mark the crossing times of the Sun through the three GLONASS orbital planes

Figure 3 shows the amplitude spectra of GNSS-specific 1-day EOP solution differences with respect to C04. As the year 2008 was still of poor quality for GLONASS, all amplitude spectra are based on the years 2009–2011. The spectral line around 120 days dominates the GLONASS 1-day solution in the pole coordinates. This line is much more pronounced in the  $x$ - than in the  $y$ -component (not shown here). In LOD we find strong semiannual and quarterly spectral lines in the GLONASS 1-day solutions as well as a signal with an amplitude of about  $8 \mu\text{s/day}$  at roughly 30 days. In addition there is a comparatively strong signal of about  $5 \mu\text{s/day}$  in LOD at around 7 days.

The consistency of GLONASS- and GPS-derived EOPs improves substantially when switching from 1- to 3-day solutions. Figure 4, showing the amplitude spectra of the GNSS-specific 3-day solutions, underscores this finding (note the scale differences in Figs. 3 and 4). The amplitude of about  $5 \mu\text{s/day}$  at 7 days occurs here as well in both, the GPS and GLONASS LOD values.

The annual, semiannual, 1/3-annual, and quarterly amplitudes for each EOP component should be put in relation to the standard deviations of the C04 series, nowadays about  $30 \mu\text{s}$  in  $x$  and  $y$  and about  $15 \mu\text{s/day}$  for LOD (Bizouard and Gambis 2011). The values show that the GLONASS spectral lines, in particular the one at 3 cpy for polar motion and the associated rates, are large compared to the GPS lines and thus artificial. In polar motion, the strongest spectral lines are at 1 and 3, in LOD at 2 and 4 cpy. The values underscore that polar motion rates derived from 1-day solutions (be they GLONASS- or GPS-only) are not useful. The corresponding 3-day estimates agree, however, very well with the C04 series.

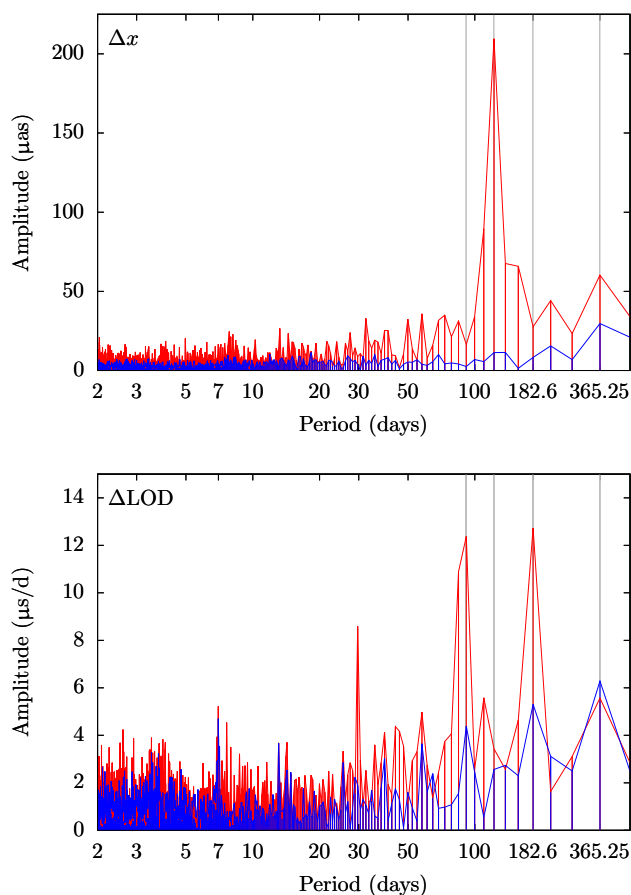


**Fig. 3** Amplitude spectra of 1-day EOP solution differences with respect to C04 for GLONASS (red) and GPS (blue). *Top*  $x$ -component, *bottom* LOD. The vertical gray lines mark the annual period and the first three harmonics of the GLONASS draconitic year

The LOD offsets indicate how rapidly a GNSS-derived UT1-UTC would drift away from the VLBI values. The 3-day offsets are substantially smaller than the corresponding 1-day offsets, speaking clearly in favor of a 3-day analysis for LOD, as well.

Table 3 provides the conventional RMS values associated with the EOP differences with respect to the C04 values for the four solutions studied in this section and the RMS error associated with periods larger than 30 days.

The full RMS values of the GPS-only solutions are clearly better than those of the GLONASS-only solutions in both, the 1- and the 3-day solutions. Within the same solution type the 3-day solutions are better than the 1-day solutions. The improvements from 1- to 3-day solutions are largest for the GLONASS-only solutions, where the RMS is reduced by factors of 2.3 and 1.6 in  $x$  and  $y$ , by factors of 4.3 and 6.4 in  $\dot{x}$  and  $\dot{y}$ , respectively. The RMS values for the GLONASS-only LOD are reduced by a factor of 1.8. The improvements are less pronounced for GPS-only solutions, but there are clear reductions, as well.

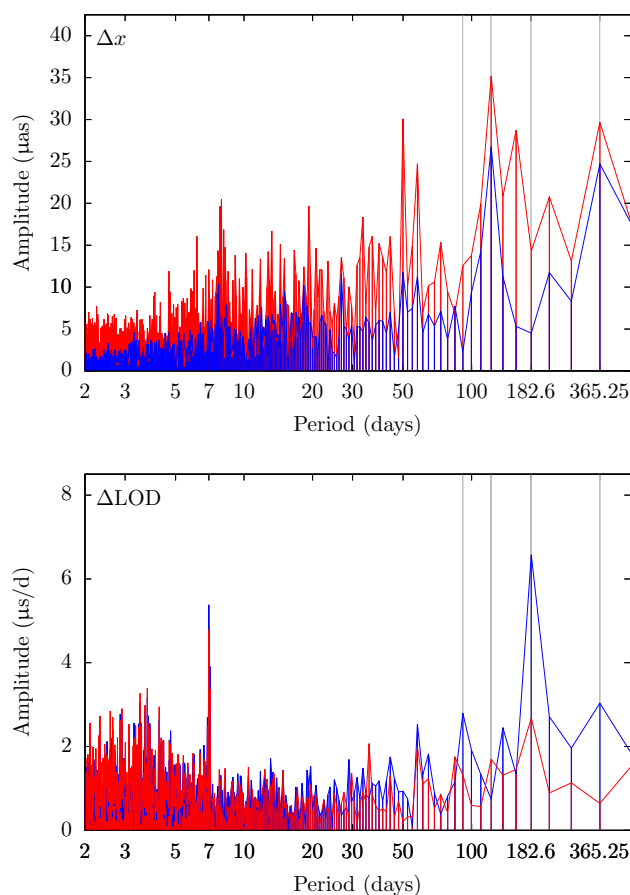


**Fig. 4** Amplitude spectra of 3-day EOP solution differences for GLONASS (red) and GPS (blue). *Top*  $x$ -component, *bottom* LOD

**Table 3** Effect of the arc length on the RMS values of the EOP solutions 2009–2011; units are  $\mu\text{as}$  for polar motion,  $\mu\text{as/d}$  for rates,  $\mu\text{s/d}$  for LOD; offsets removed

Periods included	EOP	R1	G1	R3	G3
All	$x$	238	66	103	54
	$y$	152	71	95	56
	LOD	35	22	19	20
	$\dot{x}$	585	218	136	107
	$\dot{y}$	990	244	154	113
>30 days	$x$	151	38	68	42
	$y$	76	46	65	45
	LOD	18	10	4	8
	$\dot{x}$	385	134	18	9
	$\dot{y}$	860	150	26	8

Table 3 shows a much more pronounced reduction from the 1- to the 3-day solutions in the low-pass part of the solutions. For GLONASS-only solutions the RMS values are reduced by factors of 21 and 33 in  $\dot{x}$  and  $\dot{y}$ , respectively. For the GPS-only solutions the corresponding values are 15

and 19. Less significant reductions from the 1- to 3-day solutions are nevertheless clearly visible for LOD and the pole coordinates  $x$  and  $y$ . These values document the reduction of the amplitudes of the spurious spectral lines. For all solutions the use of long arcs is mandatory, if high-quality polar motion rates are important.

The results of this section may be summarized for the 1-day solutions as follows: (a) the GLONASS-derived polar motion rates are heavily contaminated by systematics; rapid changes of up to 2 mas/d occur in  $\dot{y}$  when the Sun crosses one of the orbital planes; the directions of the changes differ for North–South and South–North crossings; (b) the  $x$ -coordinate of polar motion shows a similar pattern as  $\dot{y}$  and the  $y$ -coordinate a similar one as  $\dot{x}$ ; and (c) the rapid changes of the  $x$ -estimates at the crossing times are of the order of up to 0.5 mas.

The main findings for the 3-day solutions are as follows: (a) the spurious variations in the polar motion rates virtually disappear; (b) the systematic errors in the polar motion coordinates of GLONASS-only solutions are substantially reduced; and (c) when analyzing GLONASS-only data, multi-day solutions are essential to obtain high-quality EOPs. The offsets of the polar motion coordinates (not of their rates for the 1-day solutions) and of the LOD values are within the error bars of the C04 series.

## 5 Combined 1- and 3-day solutions

In this section the 1- and 3-day solution series C1, Cx, and C3 are studied. The Cn series will be considered separately in Sect. 6. As opposed to Sect. 4 all solutions discussed in this section are combined GPS/GLONASS solutions, with a marginal GLONASS influence between 2002 and 2008, and a growing one since 2008, network-wise and satellite-wise.

Let us distinguish four time periods:

- **Period 0: 1994–1999:** the tracking network was still developing and the solutions have not yet reached the highest possible accuracy for scientific studies.
- **Period I: 2000–2008:** the solutions are stable and accurate. They are dominated by GPS, even though GLONASS started contributing in 2002.
- **Period II: 2009–2011:** the solutions are stable and accurate; the impact of GLONASS is growing rapidly.
- **Period III: 2012–2013:** the solutions are stable and accurate, more than half of the observations stem from combined GPS/GLONASS receivers.

Subsequently, the focus is on periods I to III. The geocenter coordinates determined in CODE REPRO-2 will be

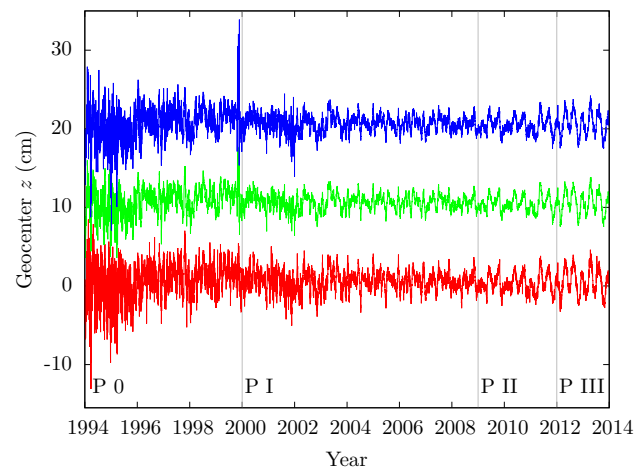


**Fig. 5** Geocenter  $z$ -coordinate from combined GPS/GLONASS solutions; C1 (red), Cx (green, shifted by 10 cm), C3 (blue, shifted by 20 cm)

analyzed in Sect. 5.1, the EOP differences in Sect. 5.2, and the orbit quality in Sect. 5.3.

### 5.1 The geocenter estimates

No substantial differences were seen in the estimates of the geocenter coordinates  $x$  and  $y$  in periods I, II, and III. Figure 5, illustrating the geocenter  $z$ -coordinate, confirms that the product quality before 2000 was not yet at the highest level. Even since then there are periodic variations in the  $z$ -coordinate of the geocenter with periods between a quarter and a full year. The amplitudes of these variations increase substantially around the first quarter of 2011. We attribute this growth to the rapid completion of the GLONASS constellation during this time period.

Figure 6 shows the amplitude spectra of the  $z$ -component. The most prominent change from period to period is the growing amplitude at 3 cpy, from 4 to 5 mm in period I, to 8–10 mm in period II, and to 16–18 mm in period III. This growth is neither of geophysical origin nor seen by SLR, but correlates with the increasing influence of GLONASS in the combined solution. It must be attributed to a deficiency of the classical empirical CODE orbit model ECOM with five parameters for the GLONASS satellites. The figures also show that the amplitude of the annual signal grew from about 4 mm to about 7–8 mm. As opposed to that the amplitudes at 5 and 7 cpy substantially decreased in time.

Table 4 contains the RMS values associated with the solutions C1, Cx, and C3 in period III. This time period was chosen because the geocenter motion in  $z$  showed the largest variations. As in Table 2 we provide the total RMS, the RMS associated with the high-pass part, and the RMS associated with the low-pass part. One more digit was provided for the high-pass RMS values to illustrate that the expected reduction of the RMS by the factor of  $\sqrt{3}$  from the C1 to the C3

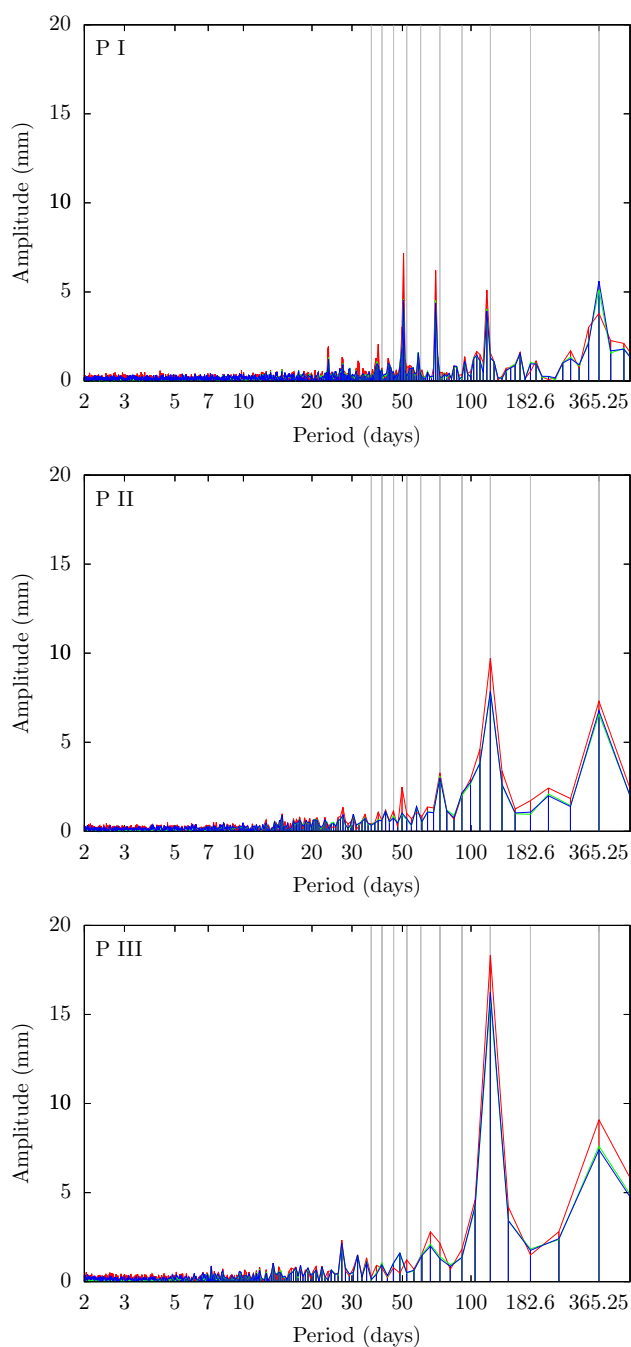


**Fig. 6** Amplitude spectra of geocenter  $z$ -component from combined GPS/GLONASS solutions C1 (red), Cx (green), and C3 (blue). *Top* period I, *center* period II, *bottom* period III

solution is the same as in Table 2. Table 4 also shows that Cx has the statistical characteristics of a 1-day solution, in particular where the high-pass part of the geocenter is concerned. We saw a clear improvement in the low-pass part of the geocenter from 1- to 3-day solutions in Table 2, which we attributed to the arc length. Such a gain cannot be seen in Table 4, which is most likely due to the much stronger global

**Table 4** Effect of the arc length on the RMS of the geocenter series for period III (2012–2013); units are mm

Periods included	Coord	C1	Cx	C3
All	$x$	6	6	5
	$y$	5	4	4
	$z$	17	16	16
<30 days	$x$	2.6	2.5	1.7
	$y$	2.6	2.6	1.7
	$z$	4.3	3.6	3.1
>30 days	$x$	5	5	5
	$y$	4	4	4
	$z$	17	16	15

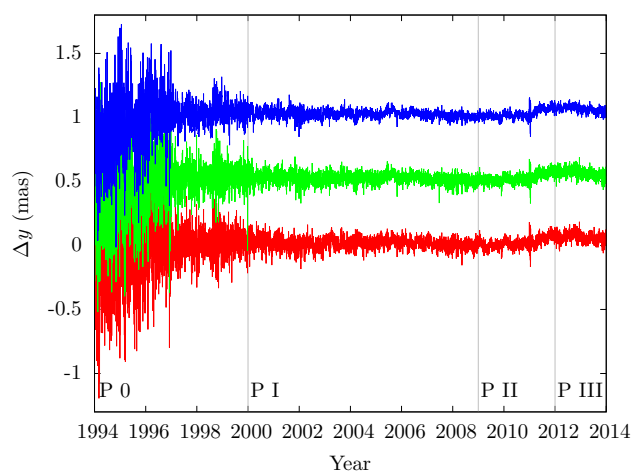


**Fig. 7** Polar motion  $y$  differences from combined GPS/GLONASS solutions; C1 (red), Cx (green, shifted by 0.5 mas), C3 (blue, shifted by 1.0 mas)

network in REPRO-2 compared to the 92 receiver network in Sect. 3.

## 5.2 The EOP estimates

Figure 7 shows the differences of the polar motion component  $y$  with respect to the C04 values as a function of time. These differences were comparatively large prior to the year 2000. Afterwards they are small, of the order of the standard deviations of the C04 polar motion series. One can also recognize that the short period variations of the differences are smaller for the C3 than for the C1 and Cx series. The standard deviation of the C3 series is by about 20–25 % smaller than that of the C1 series.

The amplitudes and offsets of the EOP differences with respect to C04 for the C1, Cx, and C3 solutions for the three defined time periods were inspected. The inspection shows that the C1 rate estimates  $\dot{x}$  and  $\dot{y}$  are of inferior quality compared to those derived from a true 3-day solution. The

$y$ -offset of the pole is about  $20 \mu\text{as}$  for periods I and II, about  $65 \mu\text{as}$  in period III. This displacement with respect to the previous periods is illustrated by Fig. 7. As our series are homogeneous with respect to processing and reference frame realization, the displacement is most likely due to the C04 series. The realization of the network in our solutions is based on an ensemble of ITRF sites, which is not identical with the official ITRF used in the IGS. We, therefore, assume that differences between the reference frame realizations in the C04 and our series caused the offsets of the C1, Cx, and C3 solutions with respect to IERS 08 C04 since early 2011. The issue needs further investigation.

The LOD offsets and the amplitudes at 1 to 4 cpy (not shown here in order to save space) document that GNSS, as all other satellite-geodetic methods, is not capable of establishing UT1-UTC. Theoretically, one would obtain a GNSS-derived UT1-UTC relative to a starting epoch by summing up the daily LOD estimates. The offsets in LOD tell how rapidly such a UT1-UTC series would drift away from the VLBI-established values. These offsets, i. e., the rates in UT1-UTC, are of the order of  $5 \mu\text{s/day}$  corresponding to approximately  $1.8 \text{ ms/year}$ .

All components of EOP discussed so far are represented at the same level of quality by all three solution series. No significant influence of the arc length can be detected, which is quite different for the polar motion rates. The drastic improvement of the GNSS-derived polar motion rates from the 1-day solution C1 to the 3-day solutions Cx and C3 is illustrated by Fig. 8 for  $\dot{x}$ . The figure moreover shows the increase of the amplitude at 3 cpy from period to period. Compared to C1 the amplitudes of the C3 spectral lines are negligible. The Cx solution lies in between C1 and C3, but only the C3 solution offers high-quality polar motion rates. The Cx series improves the consistency with the C04 reference series by a factor of two by only increasing the length of the orbit arcs but keeping offsets and rates for polar motion independent for each of the 3 days. A further significant improvement is possible by introducing the continuity condition on EOPs.

Figure 9 illustrates the LOD differences in the three periods. The main features of the LOD estimates in the GPS-only solution in Fig. 4 (bottom) and in the combined solutions in Fig. 9 (center) are consistent. The LOD differences substantially differ in the three time periods. Some of the differences (e. g., at 7, 14, and 182.5 days) may in part be caused by the C04 reference. More investigations are needed in this respect. The RMS values of the solutions will be discussed at the end of Sect. 6.

### 5.3 The orbit quality

It is problematic to assess the quality of orbits, because there is no suitable external reference available. The IGS combined

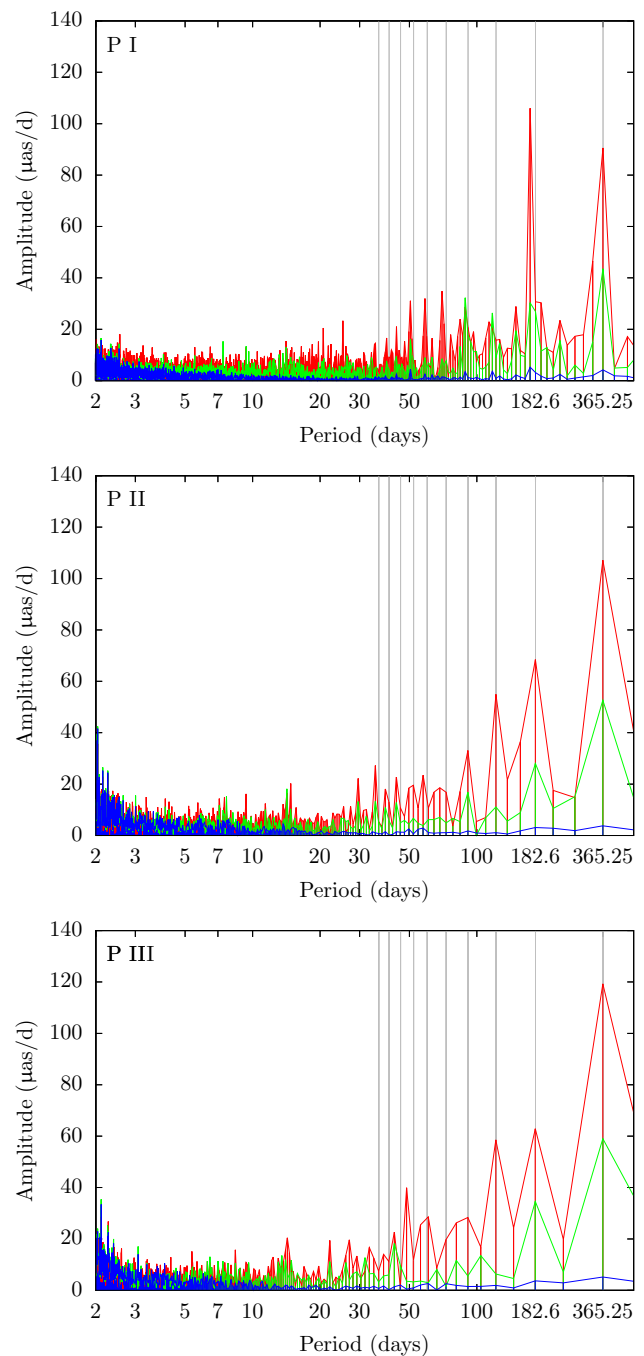


**Fig. 8** Amplitude spectra of polar motion rate  $\dot{x}$  from combined GPS/GLONASS solutions C1 (red), Cx (green), and C3 (blue). Top period I, center period II, bottom period III

orbits are not appropriate for that purpose, because their input series are based on a variety of different orbit models. Therefore, one can only check internal consistency or use SLR as a validation tool, which will be done in Sect. 7. In this section the focus is on consistency.

We define the orbit misclosure of two sets of orbits of the same type referring to days  $i$  and  $i + 1$  at the boundary of days  $i$  and  $i + 1$  as the RMS value  $m_{i,i+1}$  of the orbit differences

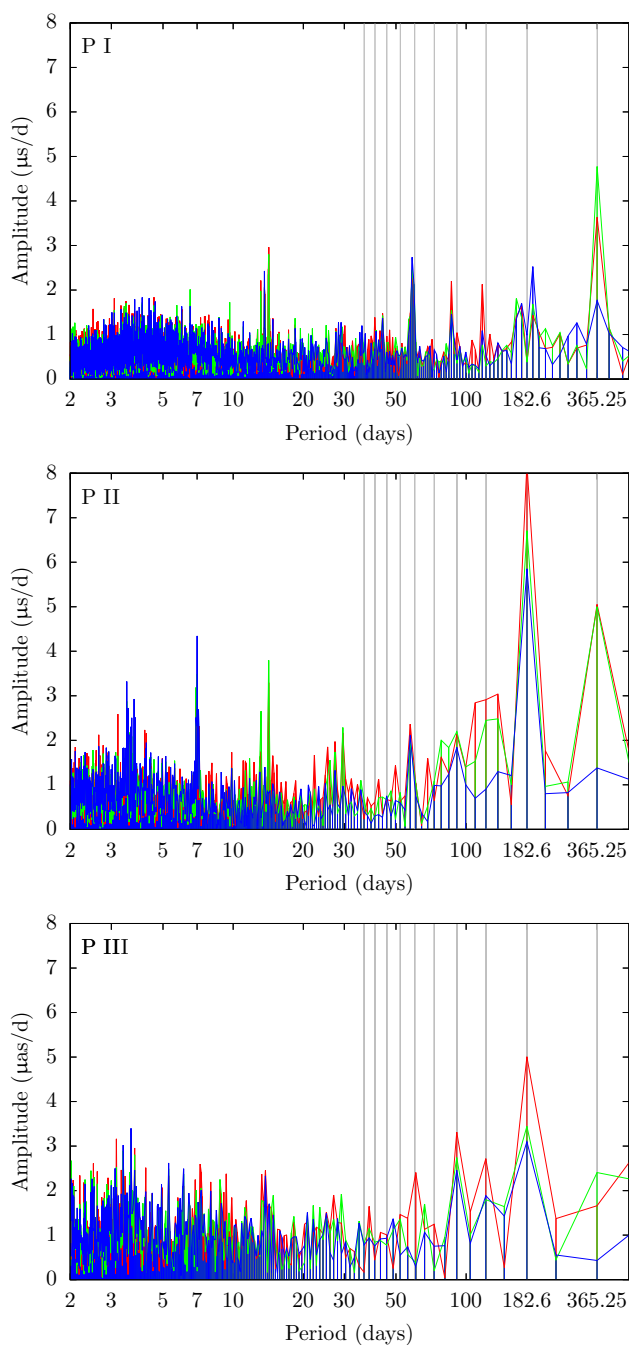


**Fig. 9** Amplitude spectra of LOD from combined GPS/GLONASS solutions C1 (red), Cx (green), and C3 (blue). *Top* period I, *center* period II, *bottom* period III

$$m_{i,i+1} = \sqrt{\frac{\sum_{s=1}^n |\mathbf{r}_{s,i+1} - \mathbf{r}_{s,i}|^2}{n}}, \quad (2)$$

where  $n$  is the number of satellites available on both days,  $\mathbf{r}_{s,i+1}$  the orbit position of satellite  $s$  based on the orbit of day  $i + 1$ , and  $\mathbf{r}_{s,i}$  the orbit position of the same satellite  $s$

**Table 5** Orbit misclosures at day boundaries in the inertial system in mm; period I is based on the years 2002–2008 because of missing GLONASS contributions in the years 2000 and 2001 in the CODE analysis

Sol	GNSS	Period I	Period II	Period III
C1	GPS	72	65	68
C1	GLO	218	115	110
Cx	GPS	40	27	31
Cx	GLO	71	30	30
C3	GPS	41	28	32
C3	GLO	72	31	31

based on the orbit of day  $i$ . Both orbit positions refer to the boundary epoch between days  $i$  and  $i + 1$ .

Satellite positions can be compared in the inertial or in the Earth-fixed coordinate system. When comparing them in the inertial system, one checks the consistency of the orbit parameters. When comparing the satellite positions in the terrestrial system one checks in addition the consistency of the EOPs on both days. Here, we only consider the misclosures in the inertial system.

Table 5 shows the mean values of the orbit misclosures for the C1, Cx, and C3 solutions, separately for GPS and GLONASS, and separately for the three periods I, II, and III. The misclosures from the Cx and C3 solutions are very similar, within 1 mm of each other. This result was expected, because the orbit parameterization is the same for Cx and C3. The differences are substantial between C1 on the one hand and Cx and C3 on the other hand. This had to be expected, as well, because Cx and C3 orbits stem from continuous 3-day arcs, sampled at a distance of half a day from the midpoint of the arc. The Cx and C3 solutions of days  $i$  and  $i + 1$  thus share 2 days of observations, namely from days  $i$  and  $i + 1$ . This fact is often used as an argument against the use of overlapping 3-day solutions. The comparison of the misclosures in Table 5 indicates, however, that the mean misclosures of the Cx and C3 orbits are about a factor of 2 smaller, thus closer to the misclosures of real orbits, which are by definition zero. Small misclosure values are often advantageous in practice, when observation periods cross day boundaries.

## 6 Non-overlapping 3-day solution

The 3-day solutions discussed in Sects. 4 and 5 are based on overlapping observation intervals. As the parameters of subsequent days are not independent, the resulting parameter time series are difficult to interpret. In the light of this criticism often raised against 3-day solutions we, therefore, construct non-overlapping 3-day solutions, as well. Such parameter series may be easily derived from the C3 solu-

tions by just extracting the values for every third day. Three different non-overlapping EOP and geocenter series may be generated in this way. Each new series has a time resolution of 3 days. We did not include spectra of these sampled EOP and geocenter series, because they are close to undistinguishable from the conventional C3 spectra in the range above 6 days (the shortest period in a spectrum based on a 3-day spacing). This reduction of the time resolution is, however, a disadvantage of the sampled C3 solutions.

The information stored for the C3 solutions allows the reconstruction of time series of EOP parameters based on adjacent, non-overlapping time intervals. One may, therefore, extract the EOP information referring to 12h of the first, second, and third day of the solution  $C3_i$  and then the same information referring to 12h of the first, second, and third day of the solution  $C3_{i+3}$ , etc. Three such time series may be generated, but only one should be used in the analysis. The EOP with 1-day time resolution referring to non-overlapping and, therefore, independent 3-day solutions, are labeled Cn. Using the same criteria as in the previous two sections, we found that the quality of these 3-day solutions based on non-overlapping 3-day solutions are closer to the quality of the overlapping 3-day arcs and that they are clearly superior to the 1-day solutions in the long-period part of the spectra.

Figure 10 shows the spectra of the polar motion rate  $\dot{y}$  differences with respect to C04 for the C1, Cx, C3 and one of the non-overlapping Cn series with 1-day time resolution. The figure indicates that the spectra of C3 and Cn are much closer in quality than Cn and C1, at least for periods longer than 30 days. The RMS values associated with  $\dot{x}$  are 168, 126, 108, and 96  $\mu\text{as}/\text{days}$  for the C1-, Cx-, Cn-, and C3-solutions; the corresponding values for  $\dot{y}$  are 232, 134, 111, and 99  $\mu\text{as}/\text{days}$ . Figure 10 also shows that the surprisingly

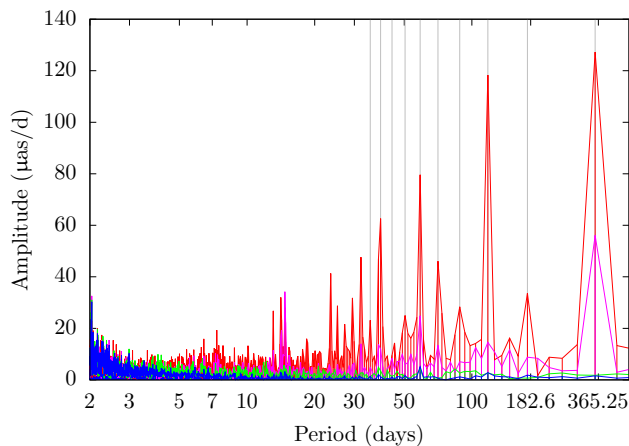


**Fig. 10** Amplitude spectra of polar motion rate  $\dot{y}$  differences with respect to C04 for the C1- (red), Cx (magenta), Cn- (green), and C3-solutions (blue) (2009–2013)

high RMS values for the 3-day solutions are due to the short-period part of the spectrum.

It is also interesting to compare the spectra of the polar motion misclosures for the four solutions represented in Fig. 10. For that purpose the time series of the previous figure had to be sampled by extracting only the values for those day boundaries separating different, subsequent 3-day arcs. The RMS values of the four series in  $x$  are 151, 96, 103, and 24  $\mu\text{as}$ , and in  $y$  216, 101, 101, and 25  $\mu\text{as}$ , for C1, Cx, Cn and C3, respectively. The RMS values are largest for the 1-day solutions; they are about 1.5 to 2 times smaller for Cx and Cn, and 15–20 times smaller for the C3 solutions. This result may surprise, at first sight. It is explained by the fact that the RMS values are dominated by the amplitudes at short periods. The main advantage of the Cn solutions is their independence and their excellent performance in the range of periods above, let us say, 30 days.

The orbit misclosures at the 3-day boundaries of the Cn solutions are roughly of the same quality as those of C1. This is of course a disadvantage compared to the C3 solution. As the Cn series are derived from C3 and because the geocenter coordinates are modeled as constants over the 3-days, no Cn geocenter series with a daily time resolution can be generated. The spectrum of the Cn series with a 3-day time resolution is in essence that of the C3 solution.

To conclude this section we provide the RMS information of the EOP series obtained with C1, Cx, Cn (1-day resolution), and C3 in Table 6. We provide the complete RMS and the RMS of the low-pass part, where all terms with periods smaller than 30 days were removed. To exclude datum problems, the offsets of all series were removed, as well.

Let us first look at the conventional RMS values. The improvements from C1 to C3 are small in the pole coordinates (24 % in  $x$ , 23 % in  $y$ ); they are large in the polar motion rates (53 % in  $\dot{x}$ , 61 % in  $\dot{y}$ ). The RMS of the LOD estimate

**Table 6** Effect of the arc length on the RMS of the EOP solution series, periods I–III; units are  $\mu\text{as}$  for polar motion,  $\mu\text{as}/\text{day}$  for rates,  $\mu\text{s}/\text{day}$  for LOD; offsets removed

Periods included	EOP	C1	Cx	Cn	C3
All	$x$	42	40	34	32
	$y$	44	42	37	34
	LOD	28	26	25	25
	$\dot{x}$	199	136	109	94
	$\dot{y}$	246	146	111	96
>30 days	$x$	24	21	21	22
	$y$	29	25	25	25
	LOD	14	11	10	10
	$\dot{x}$	136	66	16	9
	$\dot{y}$	178	72	14	9

was reduced by 12% from C1 to C3. The differences are more important, when looking at the RMS values associated with LOD and polar motion rate in the low-pass part of the series in the bottom part of Table 6: the RMS values decrease from C1 to C3 by 29% in LOD, by factors of 15 and 20 in the polar motion rates  $\dot{x}$  and  $\dot{y}$ , respectively. The RMS values for the polar motion rates confirm Fig. 10. Note, as well, that the performance of the Cn solution is much closer to that of C3 than to that of Cx. Table 6 also shows that the C3 and Cn solutions prevent the modeling deficits in the subdaily polar motion to invade the low-pass part of the solution series.

## 7 SLR validation of GNSS orbits

SLR is an independent technique for validating and assessing GNSS orbit quality. Only two GPS satellites of Block-IIA were equipped with Laser Retroreflector Arrays (LRA) in the framework of the NAVSTAR-SLR experiment (Beard 2014), whereas all GLONASS satellites are equipped with LRAs. All GLONASS satellites are currently tracked by the network of the International Laser Ranging Service (ILRS, Pearlman et al. 2002) on a regular basis.

The SLR range residuals are computed as the differences between laser ranges and the corresponding microwave orbit positions. The station coordinates are fixed to the a priori reference frame SLRF2008. No parameters are estimated, but range bias corrections are applied as recommended by the ILRS (Sošnica et al. 2015). The SLR observations are corrected for relativistic effects, troposphere delays, and for the offset of the LRA with respect to the satellites' centers of mass.

Table 7 shows the mean SLR biases and the RMS of SLR residuals for the C1 and C3 solutions for different periods. In the case of GPS, the difference between 1- and 3-day arcs is small, at maximum 2 mm of RMS difference in period I. In periods II and III, the SLR validation of C1 and C3 solutions

gives almost the same values for the mean biases and for the RMS of the residuals. The GPS results are, however, only based on the measurements to two Block IIA satellites. For GLONASS a substantial difference is observed between the C1 and C3 solutions, especially in the early years with GLONASS contribution.

The reduction in RMS amounts to 9, 4, and 1 mm for periods I, II, and III, respectively, which corresponds to RMS improvements of 21, 9, and 3%. This improvement clearly shows that long-arc solutions are particularly advantageous for incomplete satellite constellations observed by a sparse and inhomogeneous ground network like the early GLONASS network.

From the SLR validation perspective we conclude that the orbit quality of the GLONASS satellites improves when generating 3-day arcs.

## 8 Summary and conclusions

The impact of the arc length, in particular of 1- and 3-day solutions, on GNSS analysis results was studied. Two data sets were used as test material. Both were processed using the methods applied by the CODE AC. In the first data set we used the years 2009–2011 and generated GNSS-specific 1- and 3-day solutions. From the second data set of 20 years (1994–2013) we analyzed the time interval 2000–2013, where combined GPS/GLONASS 1- and 3-day solutions were computed from 2002 onwards. In the first data set we used the geocenter coordinates and the EOPs (pole coordinates, their rates, and LOD) for quality assessment, and in the second in addition the orbit misclosures and the SLR validation. C1, Cx, Cn, and C3 solutions, as defined in Sect. 3, were analyzed.

The impact on the geocenter coordinates was studied in Sects. 4 and 5. The  $z$ -component, in particular the spurious spectral line at 3 cpy, became only about 10% smaller when switching from the 1- to the 3-day solutions. The RMS of the high-pass part of the geocenter coordinates were found to be about  $\sqrt{3}$  smaller for the 3-day than for the 1-day solutions. This gain is not directly a merit of the arc length; it is simply due to the increased number of observations in the 3- with respect to the 1-day solutions. The RMS of the low-pass part of the geocenter values estimated in Sect. 4 substantially improved with the arc length: between 20 and 36% in  $x$  and  $y$ , and around 10% in  $z$ . A comparable gain could not be found in the REPRO-2 campaign. We explain this difference with the much better network geometry in REPRO-2.

The quality of EOPs from 1-day to 3-day solutions increases dramatically for the polar motion rates  $\dot{x}$  and  $\dot{y}$ . The rates based on 3-day solutions are in general much better than those based on 1-day solutions. We have shown in our analysis that this statement is true when the ECOM is used. Figure 1

**Table 7** Mean biases and RMS of SLR residuals to GPS and GLONASS satellites; all values in mm

Per	Sol	GPS		GLONASS	
		Bias	RMS	Bias	RMS
0	C1	−9	33	−	−
0	C3	−10	32	−	−
I	C1	−16	20	−2	50
I	C3	−16	18	1	41
II	C1	−12	25	−4	38
II	C3	−13	25	−2	34
III	C1	−13	27	−4	37
III	C3	−13	27	−1	36

tells, however, that similar problems are present in virtually all 1-day solutions available for REPRO-2 ( $\dot{x}$  and  $\dot{y}$  estimates of bad quality inevitably cause degraded polar motion misclosures). Table 6 shows a clear hierarchy of quality from the C1 to the C3 solution for polar motion rates (more than a factor of 10). The same table also indicates a small quality gain for other EOPs, namely  $x$ ,  $y$ , and LOD.

This leaves us with the orbit quality, expressed by the orbit misclosures at the day boundaries. Today, the GLONASS misclosures are by about a factor of 2 worse than the GPS misclosures for the GPS/GLONASS combined C1 solutions. They are at the same level for GLONASS and GPS in the 3-day solutions C3 and Cx. The improvement from the 1- to the 3-day orbit is about a factor of 2 for GPS and 4 for GLONASS. The misclosures of the Cn solutions at the 3-day boundaries were not available over the time span of REPRO-2. Tests using a limited data set have shown that the Cn 3-day misclosures were comparable in quality with those of the C1 solutions. The SLR validation confirms the better quality of the 3-day orbits, but not to the extent expected by the orbit misclosures. We attribute this to the fact that SLR “sees” the entire arc, whereas the misclosures characterize its weakest parts at the beginning and the end.

Normal users of the CODE products, interested in highest quality satellite orbits and clocks, are best served with the 3-day solutions of type C3. These solutions offer the smallest daily orbit misclosures and the highest quality in polar motion drifts and LOD. The product is readily available and robust. It is recommended in particular for partially deployed GNSS.

Cx was and still is considered as a candidate to replace C1 as CODE’s official daily contribution to the IGS. As the same statistical arguments may be used against Cx as against C3 and as its EOP quality is not as good as that of the other 3-day solutions, the decision was postponed and the issue will be further studied.

The Cn series has the advantage that it may be generated at almost no additional computational burden from the C3 solutions. The storage requirements are small, as well. As a matter of fact, all series of geophysical interest, like EOPs and geocenter coordinates, may be extracted from C3, because the full information is stored. The EOPs may even be provided with a 1-day spacing. Their quality is promising. Future will tell whether this series, which is based on non-overlapping data spans, is of interest for science. The product currently is not recommended to normal users, because the orbit quality is not as homogeneous over its 3-day intervals as that of the C3 solution. Orbit model improvements may, however, change this assessment.

**Acknowledgments** This analysis would not have been possible without the raw data and the products made available by the ILRS (Pearlman et al. 2002) and the IGS (Dow et al. 2009). Extensive use was made, as well, of the combined space-geodetic solutions for the EOPs gen-

erated by the IERS (Dick and Thaller 2014). This coordinating and combination work is gratefully acknowledged.

## References

- Altamimi Z, Collilieux X, Métivier L (2011) ITRF2008: an improved solution of the international terrestrial reference frame. *J Geod* 85(8):457–473. doi:10.1007/s00190-011-0444-4
- Arnold D, Meindl M, Beutler G, Dach R, Schaer S, Lutz S, Prange L, Sošnica K, Mervart L, Jäggi A (2015) CODE’s new solar radiation pressure model for GNSS orbit determination. *J Geod* 89(8):775–791. doi:10.1007/s00190-015-0814-4
- Beard RL (2014) The NAVSTAR 35 and 36 laser retro-reflector experiments. In: Proceedings from the 19th international workshop on laser ranging, Annapolis, US, 27–31 Oct 2014
- Beutler G, Brockmann E, Hugentobler U, Mervart L, Rothacher M, Weber R (1996) Combining consecutive short arcs into long arcs for precise and efficient GPS orbit determination. *J Geod* 70(5):287–299. doi:10.1007/BF00867349
- Brockmann E (1997) Combination of solutions for geodetic and geophysical applications of the Global Positioning System (GPS). Geodätisch-geophysikalische Arbeiten in der Schweiz 55, Eidg. Technische Hochschule Zürich, Switzerland
- Bizouard C, Gambis D (2009) The combined solution C04 for earth orientation parameters consistent with international terrestrial reference frame 2005. *Int Assoc Geod Symp* 134:265–270. doi:10.1007/978-3-642-00860-3\_41
- Bizouard C, Gambis D (2011) The combined solution C04 for earth orientation parameters consistent with international terrestrial reference frame 2008. [ftp://hpiers.obspm.fr/iers/eop/eopc04/C04\\_guide.pdf](ftp://hpiers.obspm.fr/iers/eop/eopc04/C04_guide.pdf)
- Dach R, Hugentobler U, Meindl M, Fridez P (eds) (2007) The Bernese GPS Software Version 5.0. Astronomical Institute, University of Bern
- Dach R, Brockmann E, Schaer S, Beutler G, Meindl M, Prange L, Bock H, Jäggi A, Ostini L (2009) GNSS processing at CODE: status report. *J Geod* 83(3–4):353–366. doi:10.1007/s00190-008-0281-2
- Dick WR, Thaller D (eds) (2014) IERS annual report 2012. International Earth Rotation and Reference Systems Service. Central Bureau, Bundesamt für Kartographie und Geodäsie, Richard-Strauss-Allee-11, 60598 Frankfurt am Main, Germany, ISBN 978-3-86482-058-8
- Dow JM, Neilan RE, Rizos C (2009) The International GNSS Service in a changing landscape of Global Navigation Satellite Systems. *J Geod* 83(3–4):191–198. doi:10.1007/s00190-008-0300-3
- Gambis D (2004) Monitoring earth orientation using space-geodetic techniques: state-of-the-art and prospective. *J Geod* 78(4–5):295–303. doi:10.1007/s00190-004-0394-1
- Gambis D, Luzum B (2011) Earth rotation monitoring, UT1 determination and prediction. *Metrologia* 48:S165–S170
- Griffiths J, Ray JR (2012) Sub-daily alias and draconitic errors in the IGS orbits. *GPS Solut* 17(3):413–422. doi:10.1007/s10291-012-0289-1
- Hefty J, Rothacher M, Springer TA, Weber R, Beutler G (2000) Analysis of the first year of Earth rotation parameters with a sub-daily time resolution gained at the CODE processing center of the IGS. *J Geod* 74(6):479–487. doi:10.1007/s001900000108
- Meindl M (2011) Combined analysis of observations from different global navigation satellite systems. Geodätisch-geophysikalische Arbeiten in der Schweiz 83, Eidg. Technische Hochschule Zürich, Switzerland
- Meindl M, Beutler G, Thaller D, Jäggi A, Dach R (2013) Geocenter coordinates estimated from GNSS data as viewed by perturbation

- theory. *Adv Space Res* 51(7):1047–1064. doi:[10.1016/j.asr.2012.10.026](https://doi.org/10.1016/j.asr.2012.10.026)
- Pearlman MR, Degnan JJ, Bosworth JM (2002) The international laser ranging service. *Adv Space Res* 30(2):135–143. doi:[10.1016/S0273-1177\(02\)00277-6](https://doi.org/10.1016/S0273-1177(02)00277-6)
- Petit G, Luzum B (eds) (2010) *IERS Conventions (2010)*. Verlag des Bundesamtes für Kartographie und Geodäsie, Frankfurt am Main, Germany, IERS Conventions Centre
- Press HW, Teukolsky SA, Vetterling WT, Flannery BP (1996) *Numerical recipes in Fortran 77: the Art of Scientific Computing*, 2nd edn. Cambridge University Press, Cambridge
- Ray J, Altamimi Z, Collilieux X, van Dam T (2008) Anomalous harmonics in the spectra of GPS position estimates. *GPS Solut* 12(1):55–64. doi:[10.1007/s10291-007-0067-7](https://doi.org/10.1007/s10291-007-0067-7)
- Ray J, Griffiths J, Collilieux X, Rebischung P (2013) Subseasonal GNSS positioning errors. *Geophys Res Lett* 40(22):5854–5860. doi:[10.1002/2013GL058160](https://doi.org/10.1002/2013GL058160)
- Rebischung P, Garayt B, Altamimi Z, Collilieux X (2015) The IGS contribution to ITRF2014. Presented at the 26th IUGG General Assembly, Prague, <http://acc.igs.org/trf/Rebischung-IUGG2015.ppt>. 28 June 2015
- Sošnica K, Thaller D, Dach R, Jäggi A, Beutler G (2013) Impact of loading displacements on SLR-derived parameters and on the consistency between GNSS and SLR results. *J Geod* 87(8):751–769. doi:[10.1007/s00190-013-0644-1](https://doi.org/10.1007/s00190-013-0644-1)
- Sošnica K, Thaller D, Dach R, Steigenberger P, Beutler G, Arnold D, Jäggi A (2015) Satellite laser ranging to GPS and GLONASS. *J Geod* 89(7):725–743. doi:[10.1007/s00190-015-0810-8](https://doi.org/10.1007/s00190-015-0810-8)
- Springer TA, Beutler G, Rothacher M (1999) A new solar radiation pressure model for GPS satellites. *GPS Solut* 3(2):50–62
- Steigenberger P, Rothacher M, Dietrich R, Fritsche M, Rülke A, Vey S (2006) Reprocessing of a global GPS network. *J Geophys Res* 111:B05402. doi:[10.1029/2005JB003747](https://doi.org/10.1029/2005JB003747)
- Steigenberger P, Hugentobler U, Lutz S, Dach R (2011) CODE contribution to the first IGS Reprocessing Campaign. IAPG/TUM Technical Report 1/2011, [http://www.bernese.unibe.ch/publist/2011/artproc/CODE\\_Repro1.pdf](http://www.bernese.unibe.ch/publist/2011/artproc/CODE_Repro1.pdf)